Current Research in Microbial Sciences 7 (2024) 100247

Contents lists available at ScienceDirect

Current Research in Microbial Sciences

journal homepage: www.sciencedirect.com/journal/current-research-in-microbial-sciences

Revealing the impact of Rapamycin on the virulence factors of the *Candida haemulonii* complex

Vinicius Alves [a,1], Iara Bastos de Andrade [1,a], Dario Corrêa-Junior [a], Igor Avellar-Moura [a], Karini Passos [a], Juliana Soares [b], Bruno Pontes [b,d], Marcos Abreu Almeida [c], Rodrigo Almeida-Paes [c,d], Susana Frases [a,d,*]

[a] Laboratório de Biofísica de Fungos, Instituto de Biofísica Carlos Chagas Filho, Universidade Federal do Rio de Janeiro, Rio de Janeiro 21941-902, Brazil
[b] Laboratório de Pinças Ópticas, Instituto de Ciências Biomédicas & Centro Nacional de Biologia Estrutural e Bioimagem, Universidade Federal do Rio de Janeiro, Rio de Janeiro 21941-902, Brazil
[c] Laboratório de Micologia, Instituto Nacional de Infectologia Evandro Chagas, Fundação Oswaldo Cruz, Rio de Janeiro 21040-900, Brazil
[d] Rede Micologia RJ, FAPERJ, Rio de Janeiro 21941-902, Brazil

ARTICLE INFO

Keywords:
Candida haemulonii complex
Antifungal resistance
Rapamycin

ABSTRACT

The incidence of invasive fungal infections caused by *Candida* species is increasing, particularly in immunocompromised individuals. This increasing incidence poses a dual challenge, comprising escalating antifungal resistance and the necessity for accurate fungal identification. The *Candida haemulonii* complex further complicates these challenges due to limited identification tools. Like some other *Candida* species, infections involving this complex show resistance to multiple antifungals, requiring innovative therapeutic approaches. Rapamycin, known for its antifungal properties and immunosuppressive characteristics, was investigated against the *C. haemulonii* complex species. Results revealed a rapamycin minimal inhibitory concentration (MIC) range of 0.07 to >20 μM, with fungicidal effects in most strains. *In vitro* analyses using the rapamycin maximum plasma concentration (0.016 μM) showed reduced surface properties and decreased production of extracellular enzymes. Rapamycin also hindered biofilm formation by some strains. Even when treated at the human therapeutic dose, which is lower than the MIC, phenotypic variations in *C. haemulonii* were detected, hinting at the possible attenuation of some virulence factors when exposed to rapamycin.

1. Introduction

Invasive fungal infections caused by fungi classified within the *Candida* genus are increasingly prevalent, especially in instances linked to individuals experiencing some kind of immunosuppression (Lim et al., 2012). The therapeutic management of these infections faces two interconnected challenges: the growing occurrence of strains resistant to various classes of available antifungals and the imperative need for accurate identification of these strains (Pristov and Ghannoum, 2019; Silva et al., 2012). While *Candida auris* often stands out as an example of a notably resistant *Candida* species, there is an urgent demand in the scientific community to give more attention to an emerging and potentially perilous species, the *Candida haemulonii* complex (Gómez-Gaviria et al., 2023a)

The *C. haemulonii* complex is primarily composed by three species: *C. haemuloni, C. duobushaemulonii*, and *C. haemulonii* var. *vulnera*. Distinguishing and identifying species within the *Candida haemulonii* complex from other *Candida* species is not easily achievable through most commercially available kits. Instead, methods like Matrix-Assisted Laser Desorption/Ionization Time-of-Flight Mass Spectrometry (MALDI-TOF MS) and other molecular techniques are required (Kathuria et al., 2015) The challenge of precisely identifying the *C. haemulonii* complex is underscored by the limited number of documented cases of this species causing candidemia (Colombo et al., 2017; Kathuria et al., 2015).

Infections caused by *Candida* spp. encompass a spectrum from superficial diseases such as onychomycosis and vaginal candidiasis to more severe conditions like bloodstream infections, catheter-related fungemia, osteitis, and even outbreaks in neonatal intensive care units (Crouzet et al., 2011; Guarana and Nucci, 2018). The *C. haemulonii* complex is frequently identified in human infections; however,

* Corresponding author.
E-mail address: susanafrases@biof.ufrj.br (S. Frases).
[1] Both authors contributed equally to this work

https://doi.org/10.1016/j.crmicr.2024.100247

Available online 7 June 2024

misidentification has limited the availability of comprehensive clinical data (de Almeida et al., 2016). Clinical manifestations of *C. haemulonii* complex infections closely resemble those seen with other *Candida* species and are often prevalent in immunocompromised individuals and patients with exacerbated health conditions (Brown et al., 2012). Risk factors for systemic infections include pulmonary and renal diseases, central venous catheter use, and extended stays in intensive care units (Khan et al., 2007). Each subspecies within the complex exhibits distinct characteristics. For instance, *C. haemulonii sensu stricto* is highly associated to onychomycosis and systemic candidiasis with vascular complications, while *C. duobushaemulonii* is more associated with diabetic patients (Frías-De-León et al., 2019; Ruan et al., 2010). On the other hand, *C. haemulonii* var. *vulnera* is known to cause onychomycosis, lower extremity ulcers, and fungemia (Gómez-Gaviria et al., 2023b; Rodrigues et al., 2020).

Regarding antifungal treatment options for *Candida* spp. infections, the *C. haemulonii* complex presents a distinct challenge due to its inherent resistance to fluconazole and amphotericin B, along with the potential for resistance to echinocandins, other azoles, and terbinafine (Arendrup and Patterson, 2017; Ben-Ami et al., 2017). This multidrug resistance is intricately linked to several virulence factors, notably encompassing biofilm formation, adhesin production, hydrolytic enzymes, immune system evasion, thermotolerance, and dimorphism (Gómez-Gaviria et al., 2023b). The resistance exhibited by the *C. haemulonii* complex to the sole available antifungals constitutes a substantial threat, severely constraining treatment modalities and potentially elevating mortality rates. Furthermore, there is a looming risk of resistance dissemination, entailing dire consequences. It is paramount to innovate novel therapeutic approaches to combat this mounting public health crisis.

Rapamycin is a macrolide antibiotic initially discovered on Easter Island through the isolation of *Streptomyces hygroscopicus* (Yakupoglu and Kahan, 2003). While its original therapeutic application primarily targeted infections caused by *C. albicans*, subsequent research confirmed its immunosuppressive properties by suppressing the innate immune response, achieved through the downregulation of essential transcription factors that govern the activation and proliferation of T lymphocytes (Sehgal, 2003; Sun et al., 2005). The mode of action of rapamycin hinges on the creation of an immunosuppressive complex involving an immunophilin, the intracellular receptor FK506-binding protein-12 (FKBP12) (Chan, 2004). This rapamycin-FKBP12 complex functions as an inhibitor of the mTOR, a serine/threonine protein kinase involved in cell signaling. The mTOR pathway is activated by antigens, cytokines, and/or growth factors and plays a crucial role in regulating cell motility, growth, development, proliferation, and angiogenesis (Weichhart et al., 2018). Rapamycin is typically administered orally, either in tablet or solution form. The peak plasma concentration of rapamycin averages approximately 15 ng/mL, which is roughly equivalent to 0.016 μM (Sirolimus: Uses, Interactions, Mechanism of Action | DrugBank Online).

It was identified a signaling pathway within *C. albicans* that exhibits significant homology with FKBP12 and mTOR (Cruz et al., 2001). This discovery suggests a remarkable similarity in the mechanism of action of rapamycin between fungi and mammals. The efficacy of rapamycin as an antifungal agent hinge on the presence and interaction of these specific components: FKBP12 and mTOR. Rapamycin has also demonstrated its ability to impact *Candida auris* by disrupting the fungal cell's cell cycle, inhibiting its reproductive capacity and impairing biofilm formation (Biswas et al., 2023). Given the phylogenetic similarity between *C. auris* and *C. haemulonii* complex, it is plausible that these shared structures, which serve as targets for rapamycin, may also be present in the latter. This study aims to enhance our comprehension of rapamycin's effects against *C. haemulonii* by delving into its major virulence factors.

2. Materials and methods

2.1. Fungal strains and growth conditions

Antifungal susceptibility experiments included eight clinical strains of the *C. haemulonii* species complex preserved in the "Coleção de Fungos Patogênicos" (CFP) - INI/Fiocruz pathogenic fungal collection, with the following accession numbers and species identification (Dingle and Butler-Wu, 2013): CFP1237, CFP1239, CFP1240, CFP1243, CFP1246 (*C. haemulonii*); CFP1236, CFP1242 (*C. duobusahemulonii*); and CFP1238 (*C. haemulonii* var *vulnera*). These strains were cultured in Sabouraud Dextrose Agar (SDA) - (Kasvi, Paraná, Brazil), at 37 ºC, with subcultures conducted every seven days.

2.2. Antifungal activity

Susceptibility testing was conducted using the standardized broth microdilution technique, as outlined in document 7.3.1 by the Brazilian Committee on Antimicrobial Susceptibility Testing (BrCast), to determine the minimum inhibitory concentration (MIC). The following antifungal agents were tested: amphotericin B (AMB), fluconazole (FLC), itraconazole (ITC), 5-flucytosine (5-FC), isavuconazole (ISA), anidulafungin (ANI), and rapamycin (all from Sigma-Aldrich, St. Louis, MO, USA).

Currently, there are no specific cutoff points established for species within the *C. haemulonii* complex. Consequently, we adopted the cutoff points defined for *Candida* spp. to interpret our results due to the absence of alternative guidelines, as has been done by other authors (Ramos et al., 2020c; Silva et al., 2020). The interpretation criteria were as follows: susceptible (S) if $\leq$2 μg/ml, resistant (R) if $\geq$4 μg/ml for fluconazole (FLC); S if $\leq$0.125 μg/ml, R if $>$ 0.125 μg/ml for itraconazole (ITR); S if $\leq$ 0.06 μg/ml, R if $>$ 0.06 μg/ml for anidulafungin (ANI); S if $\leq$ 1 μg/ml, R if $>$ 1 μg/ml for amphotericin B (AMB). It is important to note that cutoff points for ISA and 5-FC are not available for *Candida* species.

2.3. Fungicidal activity

Five microliters from each well of the MIC determination plates (described previously) were inoculated onto SDA to assess the fungicidal or fungistatic nature of rapamycin's antifungal activity. The minimum fungicidal concentration (MFC) was determined based on three independent experiments, defined as the lowest drug concentration where *C. haemulonii* complex growth was absent in the SDA after incubation. A drug was categorized as fungicidal if the MFC/MIC ratio was 1 or 2; if the ratio exceeded 2, it was considered fungistatic (Almeida et al., 2023).

2.4. Evaluation of rapamycin toxicity on C. haemulonii

To assess the cell viability of *C. haemulonii* complex cells treated and untreated with rapamycin, the CyQUANT™ XTT kit (Thermo Fisher, Hillsboro, OR, USA) was employed following the manufacturer's instructions. Viable cells undergoing aerobic respiration convert the XTT compound into an orange-colored product, formazan (Andrade et al., 2023).

2.5. Growth conditions in the presence of rapamycin

One representative strain from each species within the *C. haemulonii* complex (CFP1236, CFP1238, CFP1242, and CFP1243) was selected for subsequent analyses. Two strains were included in the *C. duobushaemulonii* species, one exhibiting sensitivity and the other resistance to rapamycin (CFP1236 and CFP1242). The cells were exposed to rapamycin at a plasma concentration of 0.016 μM (Sirolimus: Uses, Interactions, Mechanism of Action | DrugBank Online) in RPMI

1640 (Life Technologies, EUA) buffered with MOPS (Sigma-aldrich, EUA) at pH 7.0 for 24 h at 37 °C.

2.6. Colony forming units (CFU) countings

To evaluate the number of colony-forming units in cells treated with a plasma concentration of rapamycin, cells were cultured as above at a concentration of 10^6 cells/mL in the absence and presence of rapamycin (0.016 μM). After 24 h of incubation, a 1:1000 dilution of these cells was prepared, and 100 μL of the diluted solution was inoculated onto petri dishes containing SDA (Kasvi, Paraná, Brazil). After 24 h, the CFU count was conducted and the results were compared between rapamycin-treated and untreated cells.

2.7. Videomicroscopy analysis

The four *C. haemulonii* selected strains were initially cultured in 15 mL of Sabouraud Dextrose broth (Kasvi, Paraná, Brazil) and incubated with agitation at 5000 rpm at 37 °C for 24 h. Subsequently, the cells were adjusted to 1×10^4 cells/mL. In a glass-bottom petri dish (35×10 mm), 100 μl of 0.01 % poly-l-lysine (Sigma-Aldrich, EUA) was added to facilitate the adhesion of the cells that would be subsequently introduced. After 40 min, 100 μL of the *C. haemulonii* cell suspensions were inoculated in the coated region of the plate. After 30 min, 5 mL of RPMI 1640 supplemented with 4 % glucose (pH 7.0) were added. Control plates were performed without the presence of the drug, while the tested groups included rapamycin at a concentration of 0.016 μM.

The culture dish was then moved to a culture chamber adapted to an inverted Eclipse TE300 microscope (Nikon) with controlled temperature (37 °C). Over a period of 60 h, phase-contrast images of the same field were captured every minute using a Retiga 2000R CCD camera (Q Imaging). Subsequently, images from each experimental condition (control and 0.016 μM rapamycin treatments) and strains used in this study were compiled into videos and analyzed using the ImageJ software (National Institute of Health, Bethesda, MD, USA). The growth area was tracked over time, where a specific region of the plate containing adhered cells was selected. The area of this region with cells was determined over time by outlining the cell-populated region using the freehand tool and measuring it with the ImageJ analysis tool. Next, plots of the growth area (μm^2) over time (h) were generated for each experimental condition. τ_{50} representing the time needed to achieve 50 % of area growth in the specific condition, was determined by fitting the data to the following equation:

$$Y(t) = a + \frac{b - a}{\left[1 + \left(\frac{t}{\tau_{50}}\right)^c\right]},$$

where a and b are respectively the top and bottom plateau values of the Y-axis and c is the slope factor. The curve fits were performed using GraphPad Prism software (GraphPad Software).

2.8. Evaluation of cell surface hydrophobicity (CSH)

C. haemulonii complex cells (10^5 yeasts/mL) were pre-treated or not with the plasma concentration of rapamycin (0.016 μM) in RPMI 1640 medium, pH 7.0, for 24 h at 37 °C. Subsequently, CSH was evaluated using a two-phase water–octane assay. A 1.2 mL suspension containing 10^8 yeasts/mL was washed with phosphate-buffered saline (PBS) (Sigma-Aldrich, São Paulo, Brazil) and thoroughly mixed with 0.3 mL of octane (Sigma-Aldrich, St Louis, MO, USA). The two solvents were allowed to separate for 15 min at room temperature. The absorbance at 600 nm (ABS_{600}) of rapamycin-treated and -untreated fungal cells in PBS without octane served as the control. The percentage of fungal cells excluded from the aqueous phase (% change in ABS_{600}), indicating relative cellular hydrophobicity, was calculated using the formula: ([ABS_{600} from control—ABS_{600} after octane overlay]/ABS_{600} from control) × 100. As per established criteria, high, moderate, and low CSH correspond to respective changes of 80–100 %, 20–80 %, and 0–20 % in ABS600 (Corrêa-Junior et al., 2023).

2.9. Detection of lipid bodies in the fungal cell

The strains (10^5 cells), comprising both those subjected to rapamycin treatment and those untreated, were fixed in paraformaldehyde and subsequently stained with 5 μg/mL Nile red (Sigma-Aldrich, St. Louis, MO, USA) for 30 min at room temperature. Following staining, the absorbance was quantified using a SpectraMax plus 384 spectrophotometer (Molecular Devices, San José, CA, USA) with an excitation wavelength of 552 nm and an emission wavelength of 636 nm. To ensure accuracy, unlabeled control and treated cells were employed as blanks, and their optical density values were subtracted from those obtained for the stained samples (de Andrade et al., 2023).

2.10. Quantification of chitin in the cell wall

Both treated and untreated cells, as described above, were labeled with 10 μg/mL of Uvitex2B (Polysciences Inc., Warrington, PA, USA) and incubated at 37 °C for 30 min. The excess dye was then removed by washing the cells three times with PBS. Fluorescence was measured using a SpectraMax plus 384 spectrophotometer with excitation at 350 nm and emission at 435 nm. Unlabeled control and treated cells were employed as blanks, and their optical density was subtracted from that of the labeled cells (Ramos et al., 2020b).

2.11. Zeta potential (ξ) and conductance measurements

Cells treated or not with the maximum plasma concentration of rapamycin (0.016 μM) were cultured in RPMI 1640 at 37 ºC for 24 h, were assessed using a NanoBrook Omni Zeta potential analyzer (Brookhaven Instruments Corp., Holtsville, NY, United States), following the method outlined by Frases et al. (2009). Ten measurements were taken for each sample at 25 °C.

2.12. Production of extracellular enzymes on agar plates

The analyses of secreted hydrolytic enzymes were performed through agar plate assays as described by Price et al. (1982) and Ramos et al. (2022).

Phospholipase activity was determined using egg yolk agar plates containing SDA (Kasvi, Paraná, Brazil), 1 M NaCl (Isofar, Duque de Caxias, Brazil), 5 mM $CaCl_2$ (Sigma-Aldrich, São Paulo, Brazil), and sterile egg (8 %) yolk emulsion, pH 7.0, as previously outlined by Price et al. (1982). Esterase production was assessed using Tween agar plates according to Aktas et al. (2002), containing peptone (0.1 %) (Becton Dickinson and Company, São Paulo, Brazil), NaCl (0.05 %) (Isofar, Duque de Caixas, Brazil), $CaCl_2$ (0.001 %) (Sigma-Aldrich, São Paulo, Brazil), agar (1.5 %) (Kasvi, Paraná, Brazil), Tween 80 (0.1 %) (Sigma-Aldrich, São Paulo, Brazil), and pH 7.0.Hemolysin activity followed the protocol outlined by Luo et al., utilizing SDA (Kasvi, Paraná, Brazil) supplemented with glucose (3 %) and sheep whole blood (7 %) (Luo et al., 2001).

The lipase assay was performed on a medium containing peptone (1 %) (Becton Dickinson and Company, São Paulo, Brazil), NaCl (5 %), $CaCl_2$ (0.01 %), agar (2 %), and tween 80 (1 %) (Elavarashi et al., 2017).

Fungal cells were cultured in RPMI 1640 with and without rapamycin for 24 h. Following this, 5 μL aliquots of a 10^6 cells/mL suspension were deposited onto the surface of the culture media for enzymatic analysis, as previously described, and then incubated at 37 °C for 7 days. The dimensions of the colony were measured in millimeters, denoted as (a), as well as the diameter encompassing both the hydrolysis/precipitation zone, also measured in millimeters, denoted as (b). For all

enzymes previously delineated, the production was quantified using the Pz value (a/b), employing the methodology detailed in prior descriptions (Price et al., 1982). The Pz value was categorized into four groups: a Pz of 1.0 indicated no production, a Pz between 0.999 and 0.700 indicated poor producers, a Pz between 0.699 and 0.400 corresponded to good producers, and a Pz less than 0.399 indicated excellent producers (Price et al., 1982). *Candida krusei* (ATCC6258) and *Candida parapsilosis* (ATCC22019) were used as controls of each culture medium.

2.13. Determination of catalase activity

Determination of catalase activity was performed using a semi-quantitative assay with slight modifications according to Figueiredo-Carvalho et al. (2017). Briefly, screw-cap tubes containing SDA were inoculated with 200 μL of a suspension of *C. haemulonii* complex cells, both treated and untreated with rapamycin, at a concentration of 10^6 cells/mL. The tubes were then incubated at 37 °C for 48 h. Following this incubation, 1 mL of a freshly prepared 1:1 mixture of 10 % Tween 80 and 30 % hydrogen peroxide was added to the cultures. The column bubble height was measured in millimeters after 5 min at room temperature. Uninoculated medium served as a negative control. A column of bubbles measuring <45 mm was classified as indicative of low catalase producers, while a column bubble exceeding 45 mm was classified as indicative of high catalase producers (Corrêa-Junior et al., 2023; Figueiredo-Carvalho et al., 2017). *Candida krusei* (ATCC6258) and *Candida parapsilosis* (ATCC22019) were used as controls.

2.14. Effect of rapamycin on C. haemulonii biofilm formation

To explore the influence of rapamycin on biofilm formation, a 100 μL cell suspension containing approximately 1×10^7 cells/mL for each of the four examined strains, both treated and untreated with rapamycin in RPMI 1640 (Life Technologies, EUA), was introduced into separate wells of a 96-well plate without agitation. After 48 h incubation at 37 °C, the wells of the microtiter plate underwent three washes with 200 μL of PBS to eliminate planktonic cells. Subsequent tests, conducted in both biological and experimental triplicates, included the evaluation of the biomass and extracellular matrix of treated and untreated (control) biofilms.

For biomass analysis, fixation with 99 % methanol for 15 min was performed, followed by staining the biofilms with a 0.4 % crystal violet solution for 20 min. After removing the excess dye, the wells were washed with 200 μL of PBS. Finally, 150 μL of 33 % acetic acid (Merck, Darmstadt, Germany) was added, and 100 μL of its supernatant transferred to a new microtiter plate. The absorbance value was then be measured at 590 nm using the SpectraMax® Plus 384 Microplate Reader from Molecular Devices (Ramos et al., 2017).

To quantify the extracellular matrix, the biofilms were stained with 0.1 % safranin and incubated at room temperature for 5 min. Following another PBS wash, the biofilms were bleached with 33 % acetic acid, and absorbance was measured at 530 nm using the SpectraMax® Plus 384 Microplate Reader from Molecular Devices (Ramos et al., 2017).

2.15. Impact of rapamycin on mature biofilm disruption

Yeast suspensions were prepared in RPMI 1640 medium at a concentration of 10^7 cells/mL. Subsequently, 200 μL of the culture was added to each well of 96-well flat-bottom polystyrene plates and incubated for 48 h at 35 °C. After 48 h of biofilm formation, the rapamycin was added to RPMI 1640 at its plasma concentration (0.016 μM) and incubated for additional 48 h. As controls, yeasts in rapamycin-free culture medium were used. Biomass and extracellular matrix were measured as described above (Ramos et al., 2022).

2.16. Statistical analyses

Statistical analysis was conducted using GraphPad Prism 9.0 software (GraphPad Software, San Diego, CA, USA) for Windows 11 or macOS Monterey (version 12.7.1). Employing suitable parametric or non-parametric tests following the confirmation of data normality through the Shapiro–Wilk test. Significance for all statistical analyses was established at a p-value < 0.05.

3. Results

3.1. Antifungal activity

The MIC values for rapamycin, FLC, 5FC, ISA, ITC, ANI, and AMB were determined against eight *C. haemulonii* strains in three independent experiments, as detailed in Table 1. Rapamycin exhibited MIC values ranging from >20 to 0.07 μM. Since there are no established cutoff points for species within the *C. haemulonii* complex, our analysis also focused on evaluating the differences in MIC among the various species of the complex. The *C. duobushaemulonii* strain was observed to have high MICs for rapamycin, FLC, and AMB. *Candida haemulonii* var. *vulnera* exhibited high MIC only for AMB. The *C. haemulonii* species displayed resistance to azoles and AMB (Table 1).

3.2. Fungicidal activity

We then assessed whether rapamycin exhibits fungicidal or fungistatic activity against *C. haemulonii* in three independent experiments, with consistent results. The Table 2 illustrates the minimum fungicidal concentration of rapamycin for the 8 strains examined in this study. Rapamycin demonstrated fungistatic activity (MFC/MIC ratio > 2) for two strains and fungicidal activity (MFC/MIC ratio ≤ 2) for six strains. Interestingly, the two strains that rapamycin demonstrated fungistatic activity are *C. duobushaemulonii*.

3.3. Evaluation of rapamycin toxicity on C. haemulonii

The XTT kit was employed to assess the cell viability of *C. haemulonii* complex cells following treatment with rapamycin. In strain CFP1239, cell viability significantly decreased at a concentration of 2.5 μM. Strains CFP1237, CFP1238, and CFP1240 exhibited reduced viability from a concentration of 0.62 μM, whereas strain CFP1236 showed reduced viability at a concentration of 0.15 μM. Conversely, strains CFP1242, CFP1243, and CFP1246 did not experience statistically significant reductions in viability after treatment (Fig. 1).

Additionally, viability was assessed on representative strains with a treatment with the plasma concentration of rapamycin. In this experiment, we performed an analysis of the CFU countings of the four representative strains of the *C. haemulonii* complex. It was observed that only strains CFP1238 and CFP1242 exhibited a statistically significant reduction in growth after treatment, according to the Student's *t*-test, with both presenting a p-value of 0.04 (Fig. 2).

3.4. Determination of growth area in C. haemulonii complex species under rapamycin influence

After treatment with the plasma concentration of rapamycin, the four representative strains of the *C. haemulonii* complex used in this study were dynamically followed over time in order to monitor their growth under the microscope. Control conditions (without rapamycin treatment) were also followed for comparisons. Notably, the introduction of 0.016 μM rapamycin resulted in a delay in growth. Specifically, the strains exhibited an extended period to achieve 50 % of the total growth area compared to their controls, as demonstrated after adjusting the curve, as demonstrated after fitting the curves and determining the τ_{50} and the difference between them for each experimental condition

Table 1
Minimum inhibitory concentrations of rapamycin, fluconazole, 5-flucytosine, isavuconazole, itraconazole, anidulafungin, and amphotericin B with activity against the *C. haemulonii* complex. Results were obtained from three independent experiments.

C. haemulonii Strain	Rapamycin	Fluconazole	5-flucytosine	Isavuconazole	Itraconazole	Anidulafungin	Amphotericin B
CFP 1236	>20 μM	4 μg/mL	0,125 μg/mL	0,06 μg/mL	0,125 μg/mL	0,03 μg/mL	8 μg/mL
CFP 1237	0,62 μM	2 μg/mL	0,125 μg/mL	0,06 μg/mL	0,5 μg/mL	0,03 μg/mL	4 μg/mL
CFP 1238	5 μM	1 μg/mL	0,125 μg/mL	0,06 μg/mL	0,06 μg/mL	0,03 μg/mL	2 μg/mL
CFP 1239	1,25 μM	1 μg/mL	0,125 μg/mL	0,06 μg/mL	0,5 μg/mL	0,063 μg/mL	2 μg/mL
CFP 1240	0,07 μM	8 μg/mL	0,125 μg/mL	0,125 μg/mL	0,25 μg/mL	0,03 μg/mL	2 μg/mL
CFP 1242	0,15 μM	4 μg/mL	0,125 μg/mL	0,5 μg/mL	0,125 μg/mL	0,063 μg/mL	4 μg/mL
CFP 1243	5–2,5 μM	4 μg/mL	0,125 μg/mL	0,06 μg/mL	0,125 μg/mL	0,03 μg/mL	2 μg/mL
CFP 1246	0,31–0,15 μM	4 μg/mL	0,125 μg/mL	0,125 μg/mL	0,25 μg/mL	0,125 μg/mL	2 μg/mL

Table 2
Fungicidal activity of rapamycin against 8 *C. haemulonii* strains, determined in three independent experiments.

C. haemulonii Strain	MFC	MFC/ MIC Ratio
CFP 1236	>20 μM	1
CFP 1237	2,5 μM	4
CFP 1238	5 μM	1
CFP 1239	1,25 μM	1
CFP 1240	0,07 μM	1
CFP 1242	0,625 μM	4
CFP 1243	2,5 μM	1
CFP 1246	0,31 μM	1

(Δt_{50}) (Fig. 3 and Table 3).

When examining the occupancy of *C. haemulonii*, both treated and untreated with rapamycin over time, it was evident that 75 % of the strains treated with rapamycin take a longer time to reach the exponential phase. Furthermore, the growth curve of the CFP1238 strain, whether treated or untreated with rapamycin, exhibits remarkable similarity (Fig. 3).

3.5. Surface properties analysis of cells: hydrophobicity, zeta potential, and conductance

Another important study involved the biophysical analysis of surface properties of cells within the *C. haemulonii* complex. In this work, three parameters were examined: hydrophobicity, Zeta potential, and conductance. The assessment of the strains predisposition to hydrophobicity was carried out by partitioning fungal cells in an octane-water solution. All strains studied in this research exhibited hydrophobicity levels ranging from low to medium, without any significant difference between control and treated (Fig. 4A). To complement the results regarding surface analysis, the measurement of Zeta potential demonstrated that only strain CFP1242 showed an increase in surface electronegativity compared to the control (p-value=0.0189, t-student test), while the other strains under investigation exhibited similar surface electronegativity in both control and treated groups (Fig. 4B). However, when evaluating conductance, reflecting the surface interaction of these fungal cells in their environment, all strains showed variations between control and treated groups. Strains CFP 1242 and CFP 1236 exhibited an increase in conductance compared to the control (Fig. 4C, p-value <0.0001 for both strains, t-student test), while strains CFP 1238 and CFP 1243 showed a decrease in conductance (Fig. 4C, p-value <0.0001 and <0.1, respectively).

3.6. Quantification of chitin and lipid bodies in fungal cells

In order to elucidate the potential impact of rapamycin on the cell wall architecture of strains within the *C. haemulonii* complex, we conducted an assay to quantify chitin content in both treated and untreated cells. Notably, among all strains studied, only CFP 1242 exhibited a statistically significant chitin content reduction in rapamycin-treated cells when compared to their control counterparts (Fig. 5A, p-value <0.0001, one-way ANOVA test).

We also assessed the presence of lipid bodies when these cells were treated with rapamycin. Our findings showed, according to the one-way ANOVA test, that strains from the *C. haemulonii* complex exhibited no significant variation between lipid body contents of control and rapamycin-treated cells (Fig. 5B).

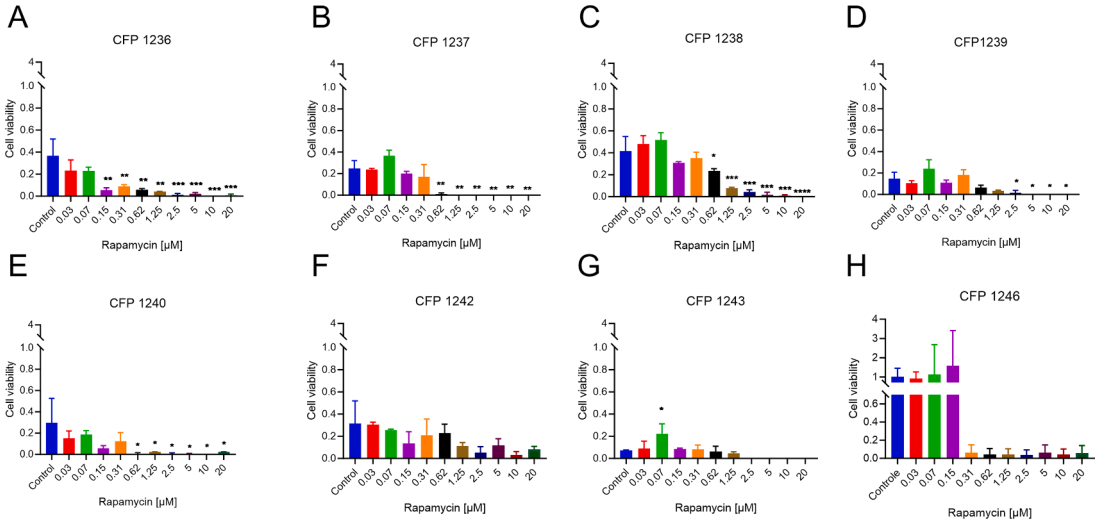

Fig. 1. The impact of rapamycin on the metabolic activity of strains of *C. haemulonii* complex was assessed using the XTT test. The results represent the mean and standard deviations of three separate experiments. Statistical significance was determined using one-way ANOVA (*p-value < 0.1; **p-value < 0.01; ***p-value < 0.001; ****p-value < 0.0001).

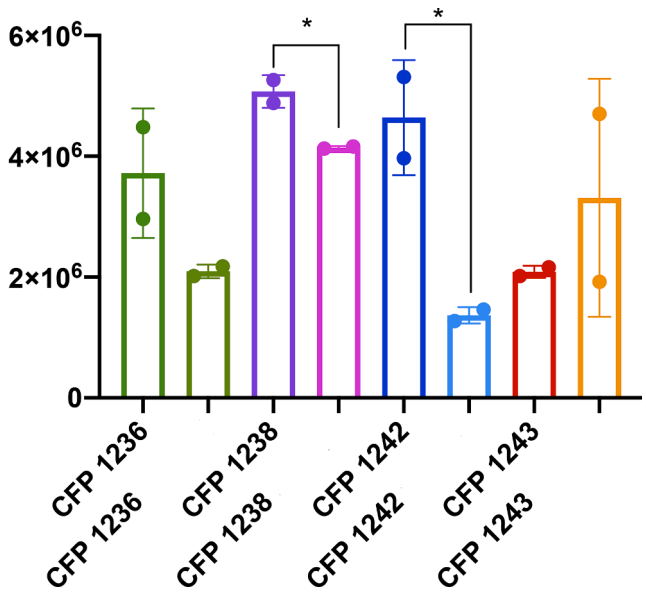

Fig. 2. Evaluation of colony forming units (CFU) of the *C. haemulonii* complex after treatment with rapamycin. The values represent the mean and standard deviation from two independent experiments. Statistical significance was determined using the Student's *t*-test (*p-value 0.04).

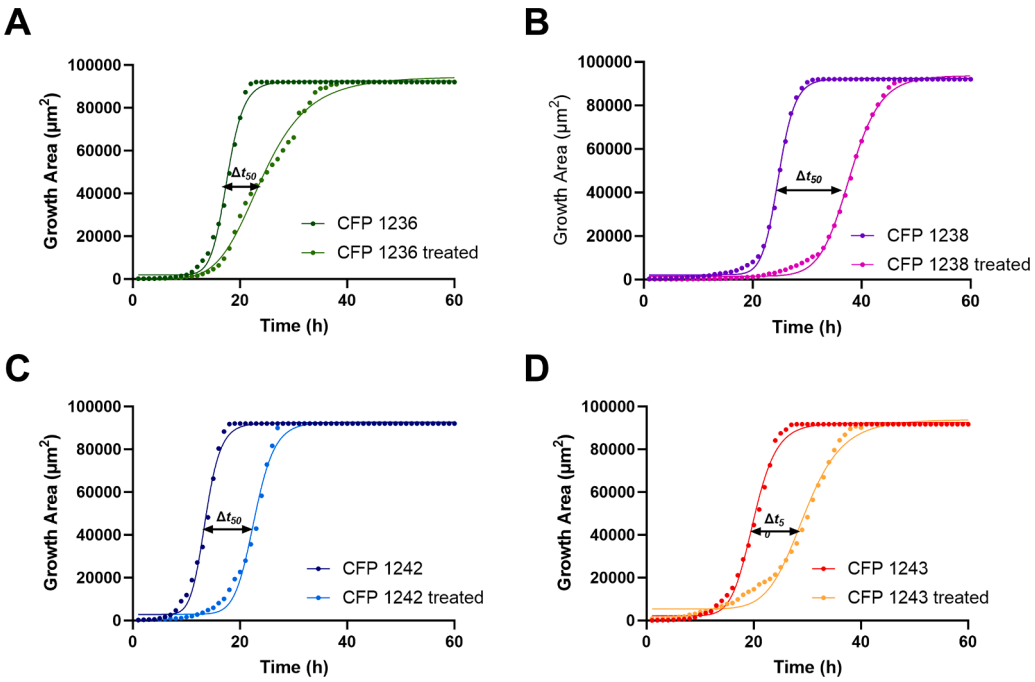

Fig. 3. Characterization of the area growth kinetics of *C. haemulonii* complex. Temporal analysis of *C. haemulonii* occupancy, comparing strains treated and untreated with rapamycin. CFP1236 (A), CFP1238 (B), CFP1242 (C), CFP 1243 (D) and all the strains (E).

Table 3
Summary of the parameters obtained for each growth curve of this study.

C. haemulonii strain	τ_{50} control (hours)	τ_{50} rapamycin (hours)	Δt_{50} (hours)
CFP1236	17.6	24.1	6.5
CFP1238	24.7	37.8	13.1
CFP1242	13.5	22.7	9.2
CFP1243	20.0	29.5	9.5

3.7. Production of extracellular enzymes

The assessment of hydrolytic enzyme secretion in both rapamycin-treated and untreated *C. haemulonii* complex strains was conducted through the agar plate test, focusing on four specific enzymes: phospholipase, esterase, hemolysin, and lipase. Notably, in the examination of phospholipase secretion, only the CFP 1243 strain exhibited a significant reduction when exposed to rapamycin treatment (p-value <0.0001, one-way ANOVA teste for all enzymatic analyses) (Fig. 6A). In the analyzed of esterase secretion, only the CFP 1236 strain exhibited a significant reduction when exposed to rapamycin treatment (p-value <0.0001) (Fig. 6B). When we analyzed hemolysin secretion, it was

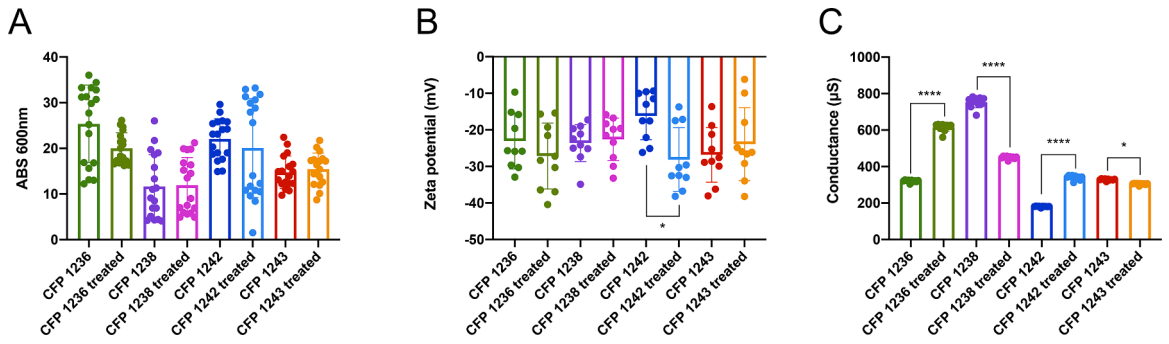

Fig. 4. Cell surface properties assessment in the *C. haemulonii* complex. Hydrophobicity was determined using the two-phase partition method (water-octane). Zeta potential and conductance were measured utilizing a Zeta potential analyzer. Hydrophobicity (A), Zeta potential (B), and conductance (C) are depicted. Each data point represents the mean value derived from three independent experiments, each conducted in triplicate. Statistical significance was determined using the Student's *t*-test (****p-value <0.0001 and *p-value 0.0189).

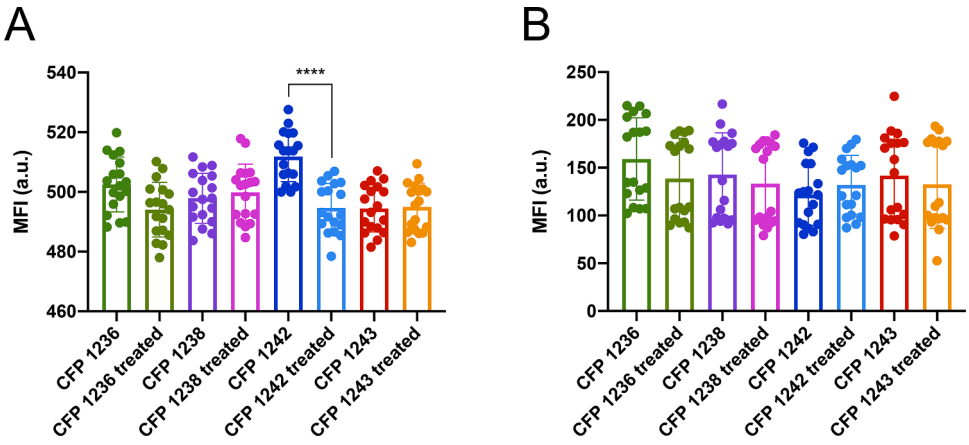

Fig. 5. Chitin and lipid body analysis in untreated and rapamycin-treated cells of *C. haemulonii* species. Cells were treated with 0.016 µM rapamycin and stained with Uvitex2B, a chitin cell wall marker (A), and Nile red, a lipid body marker (B). The results show the mean and standard deviations from three independent experiments. Statistical significance was assessed using the unpaired *t*-test (**** p-value <0.0001).

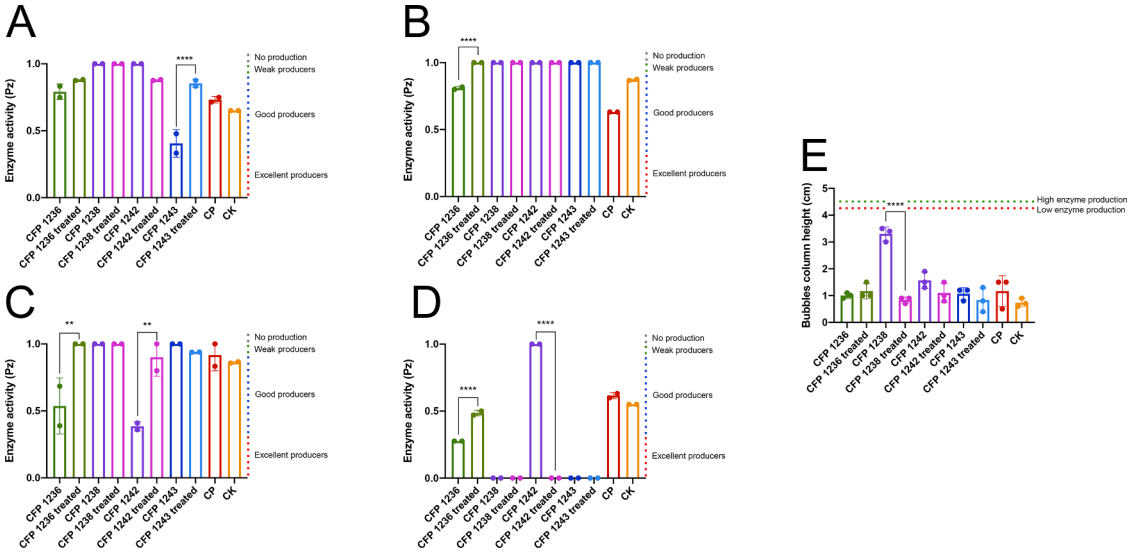

Fig. 6. Enzymes produced by the *C. haemulonii* species complex. The distribution of phospholipase (a), esterase (b), hemolysin (c), lipase (d) and catalase (e) production in each clinical isolate was shown. Note that the gray lines divide the graph according to the intensity of enzyme activity as follows: The Pz value was categorized into four groups: a Pz of 1.0 indicated no production, a Pz between 0.999 and 0.700 indicated weak producers, a Pz between 0.699 and 0.400 corresponded to good producers, and a Pz less than 0.399 indicated excellent producers. Statistical significance was determined using one-way ANOVA (**** p-value <0.0001; ** p-value= 0.0085 and 0.0039, respectively).

observed that the CFP 1236 and CFP 1242 strains had reduced enzyme secretion when the cells were treated with the plasma concentration of rapamycin (p-value 0.0085 and 0.0039, respectively) (Fig. 6C). In the culture medium designed for assessing lipase production, strains CFP 1238 and CFP 1243 did not exhibit any growth. Additionally, strain CFP 1242 failed to grow when cells were treated with rapamycin. Notably, the CFP 1236 strain experienced a significant reduction in enzyme secretion when subjected to rapamycin treatment (p-value <0.0001) (Fig. 6D). When analyzing the height of the bubble column due to the action of the catalase enzyme, we observed a statistically significant reduction in the CFP 1238 strain (p-value <0.0001) (Fig. 6E).

3.8. *Influence of rapamycin on the formation and disruption of biofilms in C. haemulonii species*

When evaluating the effect of rapamycin on the biofilm formation process, a reduction in biomass was observed only in strain CFP 1236 (Fig. 7A, p-value=0.01, one-way ANOVA test), while the other strains did not show biomass alterations in the presence of this drug. The same pattern was observed in the production of extracellular matrix, where, once again, the strain CFP 1236 exhibited a statistically significant reduction (Fig. 7B, p-value <0.1). An additional analysis was conducted to assess the influence of this drug on the deconstruction of pre-formed biofilms; however, no statistical difference was observed between evaluations of biomass (Fig. 7C) and extracellular matrix production (Fig. 7D).

4. Discussion

Concurrently, one of the major underlying conditions associated with the *C. haemulonii* species complex include organ transplantion, which requires the use of immunosuppressive drugs by the patient, including rapamycin (Silva et al., 2019). Therefore, the knowledge of the rapamycin effects in the different species of the *C. haemulonii* complex would help in a better management of patients with these infections. In this study, we obtained interesting data supporting that human achievable doses of this macrolide can modulate, differently, the virulence of the strains.

The microdilution methods for antifungals currently lack a specific cutoff point for *C. haemulonii* species. Consequently, several studies resort to comparing these results with the cutoff points established for other *Candida* species using the CLSI methodology (Ramos et al., 2022; Silva et al., 2020). In our study, we employed a similar approach. Nevertheless, we acknowledge that this approach may not be optimal, considering the diverse resistance profiles across different *Candida* species. However, this approach strives to establish a rudimentary parameter, albeit imprecise, to facilitate the interpretation of the data.

While infections attributed to species within the *C. haemulonii* complex are deemed rare, their concerning multiresistance profile to presently available antifungals, particularly amphotericin B and azoles, poses an alarming threat (Ramos et al., 2015). In our findings, it also was observed that all species within the *C. haemulonii* complex exhibited resistance to AMB, 5 out of 8 (62.5 %) were resistant to FLC and 4 out of 8 (50 %) were resistant to ITC, supporting these global findings.

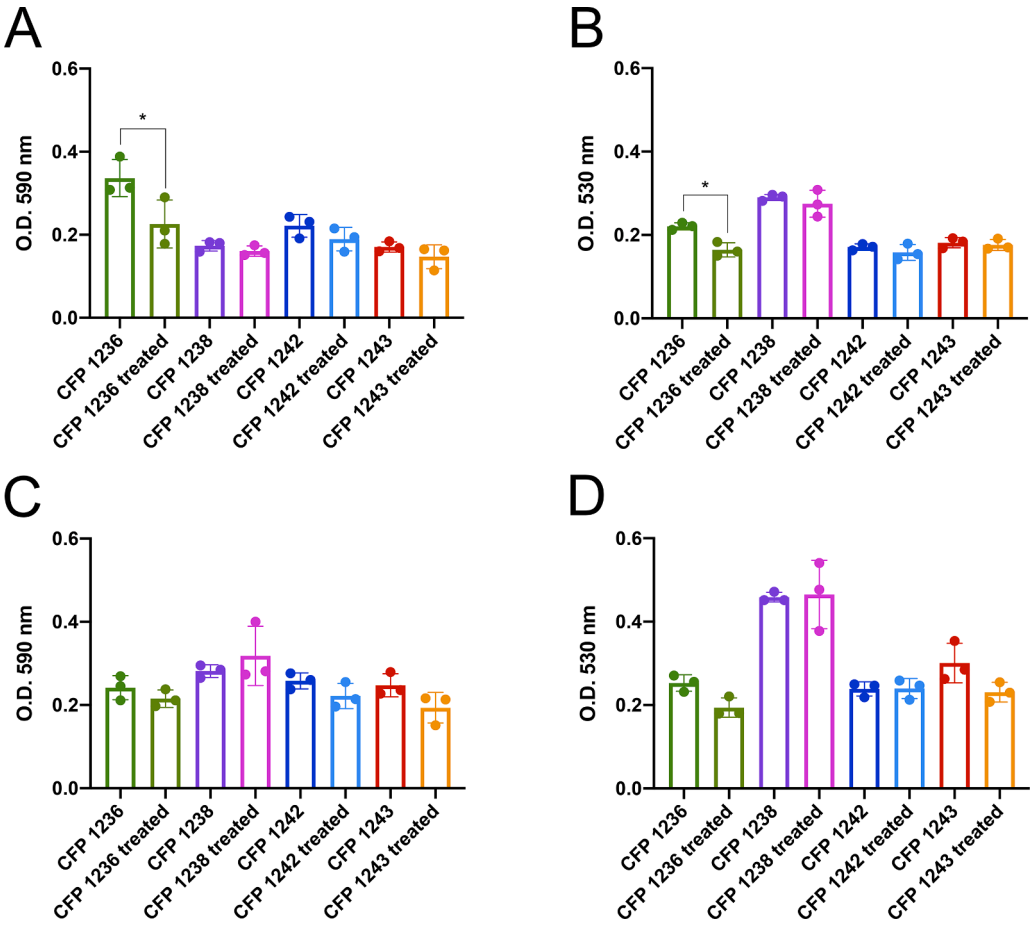

Fig. 7. Influence of rapamycin on biofilm formation and disruption in established biofilms of the *C. haemulonii* complex. Biomass quantification (A) and extracellular matrix (B) during the biofilm formation process of *C. haemulonii* complex species. Biomass quantification (C) and extracellular matrix (D) during the disruption of pre-formed biofilms by *C. haemulonii* complex species. Mean and standard deviations of three independent experiments are presented. Statistical significance was determined via unpaired t-test (*p-value =0.01).

Experiments to determine the MICs and MFCs of rapamycin in *C. albicans* and *Cryptococcus neoformans* were conducted by another group of researchers (Cruz et al., 2001). Their findings indicated that rapamycin can effectively inhibit both *C. albicans* and *C. neoformans*. In our study, we observed a fungicidal effect of rapamycin on 6 out of 8 strains (75 %) in *C. haemuloniii* strains.

These findings were validated through XTT analysis, where the cellular viability of *C. haemulonii* was examined following treatment with varying concentrations of rapamycin. It was noted that viability reduction occurred at different concentrations for each evaluated strain. Through this test, it became apparent that even in strains that exhibited resistance in the MIC assessment, such as CFP 1236, there was a notable decrease in cellular viability.

In the study conducted by Bordallo-Cardona et al.(2018), the growth kinetics of various *Candida* species were assessed based on optical density values. Their findings revealed variations in growth patterns among the different species. Similarly, our results indicate distinctions in the growth dynamics of various species within the *C. haemulonii* complex. Moreover, our data suggests that the plasma concentration of rapamycin, which is much lower than its MIC, has the potential to impair the *in vitro* growth of the *C. haemulonii* complex.

Hydrophobicity and surface properties are pivotal in the pathogenesis of *C. haemulonii* complex, impacting their ability to colonize and endure hostile environments (Ramos et al., 2020b). Rapamycin treatment did not impact the hydrophobicity of *C. haemulonii*.

On the other hand, regarding conductance, a reduction was observed in the CFP 1238 and CFP 1243 strains when comparing control and treated groups. Conversely, an increase in conductance was noted in the treated group compared to the control group in the CFP 1236 and CFP 1242 strains. Conductance is a physical-chemical property that quantifies the ability of a conductor to transmit electric current, with high conductance indicating a higher concentration of available ions in the material. These findings suggest that rapamycin may not directly alter the hydrophobicity of the strains, but rather, there is a reorganization in the relationship between charges and the surrounding environment, varying among strains. Understanding the complexities of the interaction between hydrophobicity and surface properties is imperative for unraveling the underlying mechanisms in the pathogenesis of infections by the *C. haemulonii* complex. This understanding significantly contributes to the development of more effective and precisely targeted therapeutic strategies. This information suggests that *C. haemulonii* exhibit significant variations in zeta potential and conductance on their surfaces. These variations are distinctive features of these fungi and may play important roles in their biology, potentially influencing factors such as surface adhesion, interactions with the environment, and response to external stimuli. Observing these variabilities is crucial for gaining a better understanding of the biology and behavior of these microorganisms.

Chitin is one of the pivotal carbohydrates in the fungal cell wall that maintains its structural integrity (Yang and Zhang, 2019). In addition, chitin actively participates in the modulation of immune responses and other signaling pathways (Lenardon et al., 2010). The *C. haemulonii* complex cell wall plays a central role in resistance to antifungal agents, representing a crucial component of these fungi's adaptive response to such treatments (Colombo et al., 2017; Gómez-Gaviria et al., 2023b). Alterations in the composition and integrity of the cell wall are closely linked to resistance mechanisms. A study conducted with *C. albicans* revealed the activation of a compensatory mechanism in response to caspofungin treatment, resulting in an increased amount of chitin in the cell wall. This increase can be induced in various other species, including *C. krusei, C. parapsilosis*, and *C. guilliermondii*, by enhancing the activity of the calcineurin and protein kinase C (PKC) pathways, which can be inhibited using rapamycin (Walker et al., 2013).

Our results demonstrated a considerable basal production of chitin by strains of *C. haemulonii* complex; however, at physiological rapamycin doses, no statistical difference was observed between the control and treated groups. This suggests that the amount of rapamycin reaching the bloodstream during treatment does not interfere with the composition of the cell wall structure.

Lipid bodies, primarily constituted of neutral lipids, can manifest within eukaryotic cells. These lipid bodies not only serve as energy reservoirs but also actively contribute to the formation and maintenance of cellular membranes (Ramos et al., 2020c) and coordinating a range of stress responses, encompassing the response to drugs (de Andrade et al., 2023).

Lipid bodies play a significant role in *Candida* species, providing a crucial reservoir of neutral lipids such as triglycerides and sterols that serve diverse functions in fungal cells (Dey and Maiti, 2013; Nguyen et al., 2011). The formation and accumulation of lipid bodies are dynamic and highly regulated processes that occur in response to various environmental stresses, including fluctuations in nutrient availability and the presence of antifungal agents (Suchodolski et al., 2019). However, our results did not show differences in the production of lipid bodies between control cells and those treated with the human plasma concentration of rapamycin. This finding suggests that, under the specific experimental conditions employed, rapamycin did not exert a measurable impact on the formation of lipid bodies in these specific strains.

Phospholipases participate in various biological processes, including the breakdown of phospholipids, essential components of cell membranes. In fungi, phospholipases serve several crucial functions, including nutrient acquisition, pathogenicity, and adaptation to diverse environments (Park et al., 2013). The CFP 1243 strain had its secretion reduced when treated with rapamycin. This may indicate that this drug may attenuate an important factor used by the fungus during pathogenesis.

Another important class of extracellular secreted enzymes are esterases, which catalyze the hydrolysis of ester bonds in alcohol and acid, acting better on soluble substrates. Esterases are involved in lipid digestion for nutritional purposes and, during infection, they participate in the process of adhesion and invasion of epithelial cells (Schaller et al., 2005). We observed that when cells of the CFP 1236 strain were treated with rapamycin, there was a significant decrease in enzymatic secretion, indicating again that rapamycin may attenuate the production of virulence factors by the *C. haemulonii* complex.

Fungal hemolysins are enzymes capable of promoting the lysis of red blood cells through damage to the plasma membrane, allowing the acquisition of iron, which supports the growth and development of the fungal cell. This enzyme is often related to facilitating the dissemination of *Candida* species through the bloodstream and the establishment of the infectious process (Nayak et al., 2013). In the work of Ramos et al. (2022) the production of several hydrolytic enzymes in different species of the *C. haemulonii* complex was analyzed. Their results showed that only one isolate of *C. haemulonii* var. *vulnera* showed excellent hemolytic activity, which corroborates the findings of our study. However, this species, when treated with rapamycin, had a significant decrease in the production of this enzyme. This same pattern of reduction was observed in the *C. duobushaemulonii* strain (CFP1236).

Extracellular lipases perform lipid breakdown for nutrient acquisition and adhesion to host epithelial cells (Sardi et al., 2013). Only the CFP 1236 strain (*C. duobushaemulonii*) produced lipases and this production was reduced when treated with rapamycin. Another strain of *C. duobushaemulonii* grew in the culture medium studied, but without enzymatic production. And when these cells were previously treated with rapamycin, growth was inhibited on this culture medium.

Catalase is an enzyme that plays an important role in the breakdown of hydrogen peroxide. *Candida* species are capable of neutralizing substances protecting cells from oxidative stress (Cuéllar-Cruz et al., 2014). Only the CFP 1238 strain (*C. haemulonii* var. *vulnera*) had its response to oxidative stress reduced when treated with rapamycin.

For *Candida* species, the ability to form biofilms confers significant adaptive advantages, promoting resistance to antifungal agents,

providing protection against the host's immune system, and facilitating survival in adverse environments (Pereira et al., 2021). Therefore, it is essential to investigate the impact of rapamycin on the structuring and deconstruction of biofilms produced by species of *C. haemulonii* complex.

In this study, we employed two distinct approaches: examining the effect of rapamycin on biofilm formation and, additionally, its impact on the disruption of pre-formed biofilms. It is noteworthy that the *C. haemulonii* complex demonstrates a remarkable ability to produce biofilm on various inert surfaces, constituting a prominent virulence factor associated with resistance to antifungals and candidemia, especially in individuals with medical devices (Ramos et al., 2020a).

Our findings suggest that, in already established biofilms, rapamycin may not exert substantial effects. However, in certain strains of the *C. haemulonii* complex, this drug may play a preventive role, inhibiting the complete formation of mature biofilms. These discoveries contribute to a deeper understanding of the nuances involved in the response to rapamycin treatment at different stages of biofilm formation, outlining potential therapeutic approaches to address this critical aspect of fungal virulence.

We deliberately included two strains of *C. duobushaemulonii*, with different susceptibility patterns to rapamycin. Through extensive experimentation, we observed that the strain displaying a rapamycin resistance phenotype also underwent alterations in certain virulence factors. This included a decrease in the secretion of enzymes such as esterase, hemolysin, and lipase. Furthermore, there was a notable reduction in both biomass and extracellular matrix during biofilm formation.

C. haemulonii, an emerging fungus, poses significant challenges for studies due to its limited occurrence. Despite the low number of available strains, we recognize that this limitation is inherent to the current study. However, the evaluation of virulence factors is crucial, given the prominent nature of this fungal threat. Thus, we emphasize the unique importance of our work in addressing this intrinsic challenge in the scientific landscape.

5. Conclusion

Strain-specific variations suggest potential attenuations of virulence factors under rapamycin exposure in physiological levels. These findings underscore the multifaceted response of the *C. haemulonii* complex to rapamycin, paving the way for tailored therapeutic strategies against these pathogens. *In vivo* experiments need to be performed to confirm the role of rapamycin in the pathogenesis of *C. haemulonii* complex.

Funding

This research received support from Brazilian agencies: Conselho Nacional de Desenvolvimento Científico e Tecnológico (CNPq), Coordenação de Aperfeiçoamento de Pessoal de Nível Superior - Brasil (CAPES) - Finance Code 001, and Fundação de Amparo à Pesquisa do Rio de Janeiro (FAPERJ). The authors declare no additional affiliations or financial relationships with any organization or entity that has a financial interest or conflict of interest in the subject matter or materials discussed in the manuscript, except as disclosed.

CRediT authorship contribution statement

Vinicius Alves: Methodology, Validation, Formal analysis, Investigation, Data curation, Visualization, Writing – original draft, Writing – review & editing. **Iara Bastos de Andrade:** Methodology, Validation, Formal analysis, Investigation, Data curation, Visualization, Writing – original draft, Writing – review & editing. **Dario Corrêa-Junior:** Methodology, Formal analysis, Investigation, Writing – review & editing. **Igor Avellar-Moura:** Methodology, Writing – original draft. **Karini Passos:** Methodology, Writing – review & editing. **Juliana Soares:** Methodology. **Bruno Pontes:** Methodology, Writing – review & editing, Supervision. **Marcos Abreu Almeida:** Methodology, Writing – review & editing. **Rodrigo Almeida-Paes:** Writing – original draft, Writing – review & editing, Supervision, Funding acquisition. **Susana Frases:** Visualization, Writing – original draft, Writing – review & editing, Supervision, Funding acquisition.

Declaration of competing interest

The authors declare the following financial interests/personal relationships which may be considered as potential competing interests:

Susana Frases reports financial support and equipment, drugs, or supplies were provided by National Council for Scientific and Technological Development. Susana Frases reports financial support and equipment, drugs, or supplies were provided by Carlos Chagas Filho Foundation for Research Support of Rio de Janeiro State. If there are other authors, they declare that they have no known competing financial interests or personal relationships that could have appeared to influence the work reported in this paper.

Data availability

Data will be made available on request.

References

Aktaz, E., Yigit, N., Ayyildiz, A., 2002. Esterase activity in various Candida species. J. Internat. Med. Res. 30, 322–324. https://doi.org/10.1177/147323000203000315.

Almeida, M.A., Bernardes-Engemann, A.R., Coelho, R.A., Lugones, C.J.G., de Andrade, I. B., Corrêa-Junior, D., de Oliveira, S.S.C., dos Santos, A.L.S., Frases, S., Rodrigues, M. L., Valente, R.H., Zancopé-Oliveira, R.M., Almeida-Paes, R., 2023. Mebendazole inhibits histoplasma capsulatum in vitro growth and decreases mitochondrion and cytoskeleton protein levels. J. Fungi. (Basel) 9. https://doi.org/10.3390/JOF9030385.

Andrade, I.B.De, Corr, D., Alves, V., Figueiredo-carvalho, M.H.G., Santos, M.V., Almeida, M.A., Valdez, A.F., Nimrichter, L., Almeida-paes, R., Frases, S., 2023. Cyclosporine affects the main virulence factors of cryptococcus neoformans in vitro. Journal of Fungi 9, 487.

Arendrup, M.C., Patterson, T.F., 2017. Multidrug-resistant Candida: epidemiology, molecular mechanisms, and treatment. J. Infect. Dis. 216, S445–S451. https://doi.org/10.1093/INFDIS/JIX131.

Ben-Ami, R., Berman, J., Novikov, A., Bash, E., Shachor-Meyouhas, Y., Zakin, S., Maor, Y., Tarabia, J., Schechner, V., Adler, A., Finn, T., 2017. Multidrug-Resistant Candida haemulonii and C. auris, Tel Aviv, Israel. Emerg. Infect. Dis. 23, 195–203. https://doi.org/10.3201/EID2302.161486.

Biswas, B., Gangwar, G., Nain, V., Gupta, I., Thakur, A., Puria, R., 2023. Rapamycin and Torin2 inhibit Candida auris TOR: insights through growth profiling, docking, and MD simulations. J. Biomol. Struct. Dyn. 41, 8445–8461. https://doi.org/10.1080/07391102.2022.2134927.

Bordallo-Cardona, M.Á., Sánchez-Carrillo, C., Muñoz, P., Bouza, E., Escribano, P., Guinea, J., 2018. Growth kinetics in Candida spp.: differences between species and potential impact on antifungal susceptibility testing as described by the EUCAST. Med. Mycol. 57, 601–608. https://doi.org/10.1093/MMY/MYY097.

Brown, G.D., Denning, D.W., Gow, N.A.R., Levitz, S.M., Netea, M.G., White, T.C., 2012. Hidden killers: human fungal infections. Sci. Transl. Med. 4 https://doi.org/10.1126/SCITRANSLMED.3004404.

Chan, S., 2004. Targeting the mammalian target of rapamycin (mTOR): a new approach to treating cancer. Br. J. Cancer 91, 1420–1424. https://doi.org/10.1038/sj.bjc.6602162.

Colombo, A.L., Júnior, J.N.D.A., Guinea, J., 2017. Emerging multidrug-resistant Candida species. Curr. Opin. Infect. Dis. 30, 528–538. https://doi.org/10.1097/QCO.0000000000000411.

Corrêa-Junior, D., Bastos de Andrade, I., Alves, V., Avellar-Moura, I., Brito de Souza Rabello, V., Valdez, A.F., Nimrichter, L., Zancopé-Oliveira, R.M., Ribeiro de Sousa Araújo, G., Almeida-Paes, R., Frases, S., 2023. Unveiling the Morphostructural Plasticity of Zoonotic Sporotrichosis Fungal Strains: possible Implications for Sporothrix brasiliensis Virulence and Pathogenicity. J. Fungi. (Basel) 9. https://doi.org/10.3390/JOF9070701.

Crouzet, J., Sotto, A., Picard, E., Lachaud, L., Bourgeois, N., 2011. A case of Candida haemulonii osteitis: clinical features, biochemical characteristics, and antifungal resistance profile. Clin. Microbiol. Infect. 17, 1068–1070. https://doi.org/10.1111/J.1469-0691.2011.03471.X.

Cruz, M.C., Goldstein, A.L., Blankenship, J., Del Poeta, M., Perfect, J.R., McCusker, J.H., Bennani, Y.L., Cardenas, M.E., Heitman, J., 2001. Rapamycin and less immunosuppressive analogs are toxic to Candida albicans and Cryptococcus

neoformans via FKBP12-dependent inhibition of TOR. Antimicrob. Agents Chemother 45, 3162–3170. https://doi.org/10.1128/AAC.45.11.3162-3170.2001.
Cuéllar-Cruz, M., López-Romero, E., Ruiz-Baca, E., Zazueta-Sandoval, R., 2014. Differential response of Candida albicans and Candida glabrata to oxidative and nitrosative stresses. Curr. Microbiol. 69, 733–739. https://doi.org/10.1007/S00284-014-0651-3.
de Almeida, J.N., Assy, J.G.P.L., Levin, A.S., del Negro, G.M.B., Giudice, M.C., Tringoni, M.P., Thomaz, D.Y., Motta, A.L., Abdala, E., Pierroti, L.C., Strabelli, T., Munhoz, A.L., Rossi, F., Benard, G., 2016. Candida haemulonii complex species, Brazil, January 2010-March 2015. Emerg. Infect. Dis. 22, 561–563. https://doi.org/10.3201/EID2203.151610.
de Andrade, I.B., Alves, V., Pereira, L., Miranda, B., Corrêa-Junior, D., Galdino Figueiredo-Carvalho, M.H., Santos, M.V., Almeida-Paes, R., Frases, S., 2023. Effect of rapamycin on Cryptococcus neoformans: cellular organization, biophysics and virulence factors. Future Microbiol. 18 https://doi.org/10.2217/FMB-2023-0097.
Dey, P., Maiti, M.K., 2013. Molecular characterization of a novel isolate of Candida tropicalis for enhanced lipid production. J. Appl. Microbiol. 114, 1357–1368. https://doi.org/10.1111/JAM.12133.
Dingle, T.C., Butler-Wu, S.M., 2013. Maldi-tof mass spectrometry for microorganism identification. Clin. Lab. Med. 33, 589–609. https://doi.org/10.1016/J.CLL.2013.03.001.
Elavarashi, E., Kindo, A.J., Rangarajan, S., 2017. Enzymatic and non-enzymatic virulence activities of dermatophytes on solid media. J. Clin. Diagn. Res. 11, DC23–DC25. https://doi.org/10.7860/JCDR/2017/23147.9410.
Figueiredo-Carvalho, M.H.G., Ramos, L.D.S., Barbedo, L.S., De Oliveira, J.C.A., Dos Santos, A.L.S., Almeida-Paes, R., Zancopé-Oliveira, R.M., 2017. Relationship between the antifungal susceptibility profile and the production of virulence-related hydrolytic enzymes in brazilian clinical strains of Candida glabrata. Mediators. Inflamm. 2017. https://doi.org/10.1155/2017/8952878.
Frases, S., Pontes, B., Nimrichter, L., Viana, N.B., Rodrigues, M.L., Casadevall, A., 2009. Capsule of cryptococcus neoformans grows by enlargement of polysaccharide molecules. Proc. Natl. Acad. Sci. u S. a 106, 1228–1233. https://doi.org/10.1073/pnas.0808995106.
Frías-De-León, M.G., Martínez-Herrera, E., Acosta-Altamirano, G., Arenas, R., Rodríguez-Cerdeira, C., 2019. Superficial Candidosis by Candida duobushaemulonii: an emerging microorganism. Infect. Genet. Evol. 75 https://doi.org/10.1016/J.MEEGID.2019.103960.
Gómez-Gaviria, M., Martínez-álvarez, J.A., Chávez-Santiago, J.O., Mora-Montes, H.M., 2023. Candida haemulonii complex and candida auris: biology, virulence factors, immune response, and multidrug resistance. Infect. Drug Resist. 16, 1455–1470. https://doi.org/10.2147/IDR.S402754.
Guarana, M., Nucci, M., 2018. Acute disseminated candidiasis with skin lesions: a systematic review. Clin. Microbiol. Infect. 24, 246–250. https://doi.org/10.1016/J.CMI.2017.08.016.
Kathuria, S., Singh, P.K., Sharma, C., Prakash, A., Masih, A., Kumar, A., Meis, J.F., Chowdhary, A., 2015. Multidrug-resistant candida Auris misidentified as candida haemulonii: characterization by matrix-assisted laser desorption ionization-time of flight mass spectrometry and DNA sequencing and its antifungal susceptibility profile variability by Vitek 2, CLSI broth microdilution, and etest method. J. Clin. Microbiol. 53, 1823–1830. https://doi.org/10.1128/JCM.00367-15.
Khan, Z.U., Al-Sweih, N.A., Ahmad, S., Al-Kazemi, N., Khan, S., Joseph, L., Chandy, R., 2007. Outbreak of fungemia among neonates caused by Candida haemulonii resistant to amphotericin B, itraconazole, and fluconazole. J. Clin. Microbiol. 45, 2025–2027. https://doi.org/10.1128/JCM.00222-07.
Lenardon, M.D., Munro, C.A., Gow, N.A.R., 2010. Chitin synthesis and fungal pathogenesis. Curr. Opin. Microbiol. 13, 416–423. https://doi.org/10.1016/J.MIB.2010.05.002.
Lim, C.S.Y., Rosli, R., Seow, H.F., Chong, P.P., 2012. Candida and invasive candidiasis: back to basics. Eur. J. Clin. Microbiol. Infect. Dis. 31, 21–31. https://doi.org/10.1007/S10096-011-1273-3.
Luo, G., Samaranayake, L.P., Yau, J.Y.Y., 2001. Candida species exhibit differential *in vitro* hemolytic activities. J. Clin. Microbiol. 39, 2971–2974. https://doi.org/10.1128/JCM.39.8.2971-2974.2001.
Nayak, A.P., Green, B.J., Beezhold, D.H., 2013. Fungal hemolysins. Med. Mycol. 51, 1–16. https://doi.org/10.3109/13693786.2012.698025.
Nguyen, L.N., Hamari, Z., Kadereit, B., Trofa, D., Agovino, M., Martinez, L.R., Gacser, A., Silver, D.L., Nosanchuk, J.D., 2011. Candida parapsilosis fat storage-inducing transmembrane (FIT) protein 2 regulates lipid droplet formation and impacts virulence. Microbes. Infect. 13, 663–672. https://doi.org/10.1016/J.MICINF.2011.02.009.
Park, M., Do, E., Jung, W.H., 2013. Lipolytic enzymes involved in the virulence of human pathogenic fungi. Mycobiology. 41, 67–72. https://doi.org/10.5941/MYCO.2013.41.2.67.
Pereira, R., dos Santos Fontenelle, R.O., de Brito, E.H.S., de Morais, S.M., 2021. Biofilm of Candida albicans: formation, regulation and resistance. J. Appl. Microbiol. 131, 11–22. https://doi.org/10.1111/JAM.14949.
Price, M.F., Wilkinson, A.N.D., Gentry, L.O., 1982. Plate method for detection of phospholipase activity in Candida albicans 7–14.
Pristov, K.E., Ghannoum, M.A., 2019. Resistance of Candida to azoles and echinocandins worldwide. Clin. Microbiol. Infect. 25, 792–798. https://doi.org/10.1016/J.CMI.2019.03.028.
Ramos, L.S., Figueiredo-Carvalho, M.H.G., Barbedo, L.S., Ziccardi, M., Chaves, A.L.S., Zancopé-Oliveira, R.M., Pinto, M.R., Sgarbi, D.B.G., Dornelas-Ribeiro, M., Branquinha, M.H., Santos, A.L.S., 2015. Candida haemulonii complex: species identification and antifungal susceptibility profiles of clinical isolates from Brazil. J. Antimicrob. Chemother 70, 111–115. https://doi.org/10.1093/JAC/DKU321.
Ramos, L.S., Figueiredo-Carvalho, M.H.G., Silva, L.N., Siqueira, N.L.M., Lima, J.C., Oliveira, S.S., Almeida-Paes, R., Zancopé-Oliveira, R.M., Azevedo, F.S., Ferreira, A.L.P., Branquinha, M.H., Santos, A.L.S., 2022. The threat called Candida haemulonii species complex in rio de janeiro state, brazil: focus on antifungal resistance and virulence attributes. J. Fungi 2022 8, 574. https://doi.org/10.3390/JOF8060574. Vol.Page8, 574.
Ramos, L.S., Mello, T.P., Branquinha, M.H., Santos, A.L.S., 2020a. Biofilm formed by Candida haemulonii species complex: structural analysis and extracellular matrix composition. J. Fungi. (Basel) 6. https://doi.org/10.3390/JOF6020046.
Ramos, L.S., Oliveira, S.S.C., Silva, L.N., Granato, M.Q., Gonçalves, D.S., Frases, S., Seabra, S.H., Macedo, A.J., Kneipp, L.F., Branquinha, M.H., Santos, A.L.S., 2020b. Surface, adhesiveness and virulence aspects of Candida haemulonii species complex. Med. Mycol. 58, 973–986. https://doi.org/10.1093/mmy/myz139.
Ramos, L.S., Oliveira, S.S.C., Souto, X.M., Branquinha, M.H., Santos, A.L.S., 2017. Planktonic growth and biofilm formation profiles in Candida haemulonii species complex. Med. Mycol. 55, 785–789. https://doi.org/10.1093/MMY/MYX005.
Ramos, L.S., Silva, L.N., Branquinha, M.H., Santos, A.L.S., 2020c. Susceptibility of the Candida haemulonii complex to echinocandins: focus on both planktonic and biofilm life styles and a literature review. J. Fungi. (Basel) 6, 1–16. https://doi.org/10.3390/JOF6040201.
Rodrigues, L.S., Gazara, R.K., Passarelli-Araujo, H., Valengo, A.E., Pontes, P.V.M., Nunes-da-Fonseca, R., de Souza, R.F., Venancio, T.M., Dalla-Costa, L.M., 2020. First genome sequences of two multidrug-resistant candida haemulonii var. vulnera isolates from pediatric patients with Candidemia. Front. Microbiol. 11 https://doi.org/10.3389/FMICB.2020.01535.
Ruan, S.Y., Kuo, Y.W., Huang, C.T., Hsiue, H.C., Hsueh, P.R., 2010. Infections due to Candida haemulonii: species identification, antifungal susceptibility and outcomes. Int. J. Antimicrob. Agents 35, 85–88. https://doi.org/10.1016/J.IJANTIMICAG.2009.08.009.
Sardi, J.C.O., Scorzoni, L., Bernardi, T., Fusco-Almeida, A.M., Mendes Giannini, M.J.S., 2013. Candida species: current epidemiology, pathogenicity, biofilm formation, natural antifungal products and new therapeutic options. J. Med. Microbiol. 62, 10–24. https://doi.org/10.1099/JMM.0.045054-0.
Schaller, M., Borelli, C., Korting, H.C., Hube, B., 2005. Hydrolytic enzymes as virulence factors of Candida albicans. Mycoses. 48, 365–377. https://doi.org/10.1111/J.1439-0507.2005.01165.X.
Sehgal, S.N., 2003. Sirolimus: its discovery, biological properties, and mechanism of action. TransPlant Proc. 35, S7–S14. https://doi.org/10.1016/S0041-1345(03)00211-2.
Silva, L.N., de Mello, T.P., de Souza Ramos, L., Branquinha, M.H., dos Santos, A.L.S., 2019. New and promising chemotherapeutics for emerging infections involving drug-resistant non-albicans Candida Species. Curr. Top. Med. Chem. 19, 2527–2553. https://doi.org/10.2174/1568026619666191025152412.
Silva, L.N., Ramos, L., de, S., Oliveira, S.S.C., Magalhães, L.B., Squizani, E.D., Kmetzsch, L., Vainstein, M.H., Branquinha, M.H., dos Santos, A.L.S., 2020. Insights into the multi-azole resistance profile in Candida haemulonii species complex. J. Fungi. (Basel) 6, 1–16. https://doi.org/10.3390/JOF6040215.
Silva, S., Negri, M., Henriques, M., Oliveira, R., Williams, D.W., Azeredo, J., 2012. Candida glabrata, Candida parapsilosis and Candida tropicalis: biology, epidemiology, pathogenicity and antifungal resistance. FEMS Microbiol. Rev. 36, 288–305. https://doi.org/10.1111/J.1574-6976.2011.00278.X.
Sirolimus: uses, interactions, mechanism of action drugbank online [WWW Document], n.d. URL https://go.drugbank.com/drugs/DB00877 (accessed 11.14.23).
Suchodolski, J., Muraszko, J., Korba, A., Przemysław Bernat, Krasowska, A., 2019. Lipid composition and cell surface hydrophobicity of Candida albicans influence the efficacy of fluconazole-gentamicin treatment. 10.1002/yea.3455.
Sun, S.Y., Rosenberg, L.M., Wang, X., Zhou, Z., Yue, P., Fu, H., Khuri, F.R., 2005. Activation of Akt and eIF4E survival pathways by rapamycin-mediated mammalian target of rapamycin inhibition. Cancer Res. 65, 7052–7058. https://doi.org/10.1158/0008-5472.CAN-05-0917.
Walker, L.A., Gow, N.A.R., Munro, C.A., 2013. Elevated chitin content reduces the susceptibility of Candida species to caspofungin. Antimicrob. Agents Chemother 57, 146–154. https://doi.org/10.1128/AAC.01486-12.
Weichhart, T., Hengstschläger, M., Linke, M., 2018. Regulation of innate immune cell function by mTOR. Nat. Rev. Immunol. 15, 599–614. https://doi.org/10.1038/nri3901.Regulation.
Yakupoglu, Y.K., Kahan, B.D., 2003. Sirolimus: a current perspective. Exp. Clin. TransPlant 1, 8–18.
Yang, J., Zhang, K.Q., 2019. Chitin synthesis and degradation in fungi: biology and enzymes. Adv. Exp. Med. Biol. 1142, 153–167. https://doi.org/10.1007/978-981-13-7318-3_8.